Addition Spectra of Quantum Dots: the Role of Dielectric Mismatch

A. Franceschetti,* A. Williamson, and A. Zunger

National Renewable Energy Laboratory, Golden, Colorado 80401

Received: January 4, 2000; In Final Form: February 20, 2000

Using atomistic pseudopotential wave functions, we calculate the electron and hole addition energies and the quasi-particle gap of InAs quantum dots. We find that the addition energies and the quasi-particle gap depend strongly on the dielectric constant ϵ_{out} of the surrounding material, and that when ϵ_{out} is much smaller than the dielectric constant of the dot the electron−electron and hole−hole interactions are dominated by surface polarization effects. We predict the addition energies and the quasi-particle gap as a function of size and ϵ_{out}, and compare our results with recent single-dot tunneling spectroscopy experiments.

Recently developed single-dot tunneling spectroscopy techniques[1] have allowed for the first time the observation of atomiclike electronic states in strongly-confined semiconductor quantum dots. In these experiments, a scanning tunneling microscopy (STM) tip is positioned above a specific quantum dot, and the tunneling current−voltage spectrum is acquired by applying a bias V between the STM tip and the substrate. The tunneling conductance dI/dV shows, as a function of V, a series of sharp peaks which correspond (possibly via a scaling factor) to the electron and hole charging energies μ_N. It has been realized for some time[2,3] that the addition spectrum of semiconductor quantum dots is profoundly affected by the dielectric environment. Indeed, semiconductor quantum dots can now be made with various dielectric coatings: organic molecules,[4] other semiconductors (e.g., self-assembled dots,[5] core−shell nanocrystals,[6] lithographically-etched dots,[7] strain-induced dots[8]), or glasses.[9] In this paper, we will quantitatively predict how the addition spectra of quantum dots depend on the dielectric environment and explain the results of ref 1 in terms of microscopic quantities.

Consider the two processes described in Figure 1, where a quantum dot of dielectric constant ϵ_{in} is embedded in a material of dielectric constant ϵ_{out}. Figure 1a depicts the process of adding three electrons to an otherwise neutral quantum dot. The initial configuration of the system, of energy E_0, consists of a neutral dot in the ground state and a Fermi reservoir at the reference energy $\epsilon_{ref} = 0$. The "charging energy" μ_1 required to load the first electron into the dot is

$$\mu_1 \equiv E_1 - E_0 = \epsilon_{e1} + \Sigma_{e1}^{pol} \tag{1}$$

where E_1 is the total energy of the dot with one additional electron, ϵ_{e1} is the energy of the single-particle level e1 with respect to the reference energy ϵ_{ref}, and Σ_{e1}^{pol} is the self-energy of the additional electron interacting with its own image charge created by the dielectric mismatch at the surface of the dot.[3] The charging energy for the second electron is

$$\mu_2 \equiv E_2 - E_1 = \epsilon_{e1} + \Sigma_{e1}^{pol} + J_{e1,e1} \tag{2}$$

where $J_{e1,e1}$ is the Coulomb interaction between the two electrons. It includes a direct contribution $J_{e1,e1}^{dir}$ and a polarization contribution $J_{e1,e1}^{pol}$ arising from the interaction of one electron with the image charge of the other electron.[3] Finally, the charging energy for the third electron is

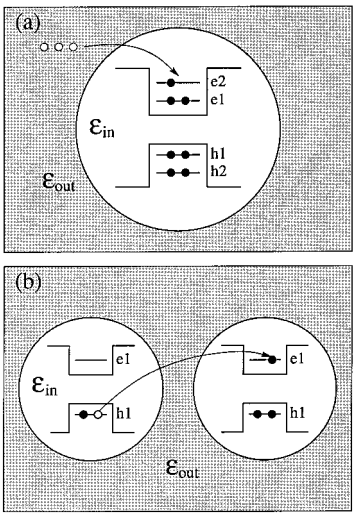

Figure 1. (a) Process of loading three electrons into an otherwise neutral quantum dot. (b) Process of removing a single electron from a dot and placing it into another dot.

$$\mu_3 \equiv E_3 - E_2 = \epsilon_{e2} + \Sigma_{e2}^{pol} + 2J_{e1,e2} - K_{e1,e2} \tag{3}$$

where $K_{e1,e2}$ is the exchange energy between two electrons with parallel spins in the e1 and e2 single-particle levels. The "addition energies" for the second and the third electrons are respectively

$$\Delta_{1,2} \equiv \mu_2 - \mu_1 = J_{e1,e1} \tag{4}$$

$$\Delta_{2,3} \equiv \mu_3 - \mu_2 = (\epsilon_{e2} - \epsilon_{e1}) + (\Sigma_{e2}^{pol} - \Sigma_{e1}^{pol}) + (2J_{e1,e2} - J_{e1,e1}) - K_{e1,e2} \tag{5}$$

Since Σ_i^{pol} and $J_{i,j}^{pol}$ depend strongly on the dielectric constant of the surrounding material, the addition energies of a quantum dot depend on its dielectric environment.

Figure 1b describes the process of removing an electron from the highest occupied orbital of a neutral quantum dot and placing it into the lowest unoccupied orbital of an identical dot (located

* Corresponding author.

10.1021/jp0000026 CCC: $19.00
Published on Web 03/25/2000

at infinite distance from the first dot). The energy required by this process ("quasi-particle gap") is the difference between the ionization potential and the electron affinity of the dot. The initial configuration, consisting of the two neutral dots in the ground state, has energy $2E_0$, while the final configuration has energy $E_1 + E_{-1}$, where E_{-1} is the energy of the quantum dot with a hole in the highest occupied orbital h1. The quasi-particle gap is then

$$\epsilon_{gap}^{qp} = E_1 + E_{-1} - 2E_0 = \epsilon_{gap} + \Sigma_{e1}^{pol} + \Sigma_{h1}^{pol} \quad (6)$$

where $\epsilon_{gap} \equiv \epsilon_{e1} - \epsilon_{h1}$ is the single-particle (HOMO−LUMO) gap. We see that the quasi-particle gap depends, via the polarization self-energies Σ_{e1}^{pol} and Σ_{h1}^{pol}, on the dielectric environment.

The effects of dielectric confinement on the excitonic gap and the charging energies of quantum dots have been addressed in the past[3,10−13] using the effective-mass approximation. Recent pseudopotential calculations[14,15] have demonstrated the importance of using an atomistic description of the quantum dot electronic structure for calculating the single-particle energy levels and the electron−hole Coulomb energies. In fact, the pseudopotential approach provides an accurate description of the wave function decay outside the quantum dot and of the interband coupling due to quantum confinement, which are required for a correct evaluation of Coulomb energies in small nanocrystals. Using pseudopotential wave functions, we discuss here the dependence of (i) the electron and hole charging energies $\mu_N = E_N - E_{N-1}$, (ii) the addition energies $\Delta_{N,N+1} = \mu_{N+1} - \mu_N$, and (iii) the quasi-particle band gap $\epsilon_{gap}^{qp} = \mu_1 - \mu_{-1}$ of InAs nanocrystals on the dielectric constant ϵ_{out} of the surrounding material. We find that for $\epsilon_{out} = 6$ our results are in good agreement with the experimental data of Banin et al.,[1] and interpret the electron and hole addition energies in terms of Coulomb and polarization contributions (eqs 1−6).

The many-particle wave function Ψ_N of a system of N electrons in the conduction band of a quantum dot can be approximated by a single Slater determinant constructed from the wave functions $\{\psi_i, i = 1, ..., N\}$ of the N single-particle states occupied by the N electrons. The corresponding total energy is

$$E_N = E_0 + \sum_i (\epsilon_i + \Sigma_i^{pol}) n_i + \sum_{i<j} (J_{i,j} - K_{i,j}) n_i n_j \quad (7)$$

where ϵ_i are the conduction-band single-particle energy levels, Σ_i^{pol} are the polarization self-energies, $J_{i,j}$, $K_{i,j}$ are the electron−electron Coulomb and exchange energies, respectively, and n_i are the occupation numbers ($\sum_i n_i = N$). The ground state wave function Ψ_N^0 corresponds to the configuration that minimizes the total energy E_N. In eq 7 we neglect (i) the coupling between different Slater determinants (i.e., configuration-interaction effects), and (ii) the response of the single-particle wave functions ψ_i to the electrostatic field (i.e., self-consistent effects). In other words, we calculate Σ_i^{pol}, $J_{i,j}$, and $K_{i,j}$ using the single-particle wave functions of a neutral dot in the ground state. This perturbative approach has been tested in the case of excitons both versus self-consistent calculations[15] and versus configuration-interaction calculations.[16] It was found that perturbation theory is sufficiently accurate for zero-dimensional structures in the strong-confinement regime.[15−17]

The single-particle energies ϵ_i and wave functions $\psi_i(\mathbf{r},\sigma)$ are given by the solution of the Schrödinger equation:

$$[-\nabla^2 + V_{ps}(\mathbf{r})]\psi_i(\mathbf{r},\sigma) = \epsilon_i \psi_i(\mathbf{r},\sigma) \quad (8)$$

The pseudopotential of the quantum dot $V_{ps}(\mathbf{r})$ is obtained from the superposition of screened atomic potentials, which are fitted[14] to the bulk experimental optical transition energies and effective masses, as well as the surface work function. Spin−orbit coupling is fully included in the solution of the Schrödinger equation.

The interelectronic energies $J_{i,j}$ are given by

$$J_{i,j} = e\sum_\sigma \int |\psi_i(\mathbf{r},\sigma)|^2 \Phi_j(\mathbf{r})\, d\mathbf{r} \quad (9)$$

where $\Phi_j(\mathbf{r})$ is the electrostatic potential energy due to a charge distribution $\rho_j(\mathbf{r}) = e\sum_\sigma |\psi_j(\mathbf{r},\sigma)|^2$ in a dielectrically inhomogeneous medium. $\Phi_j(\mathbf{r})$ satisfies the Poisson equation:

$$\nabla\cdot\epsilon(\mathbf{r})\nabla\Phi_j(\mathbf{r}) = -4\pi\rho_j(\mathbf{r}) \quad (10)$$

where $\epsilon(\mathbf{r})$ is the (position-dependent) macroscopic dielectric constant of the system. The Poisson equation is solved on a real-space grid using a finite-difference discretization of the gradient operator. The boundary conditions are obtained from a multipole expansion of the electrostatic potential.[15] The dielectric constant $\epsilon(\mathbf{r})$ changes smoothly from ϵ_{in} to ϵ_{out}, with a transition region of the order of the interatomic bond length. The interelectronic energy $J_{i,j}$ can be separated into two contributions: (a) the direct Coulomb energy $J_{i,j}^{dir}$, which corresponds to the interaction between two electrons in the quantum dot as if the dielectric constant was uniform throughout the system, and identical to the macroscopic dielectric constant of the quantum dot; and (b) the polarization energy $J_{i,j}^{pol}$ which accounts for the effects of the dielectric mismatch at the interface between the dot and the surrounding material, and the ensuing surface polarization charge.

The polarization self-energies Σ_i^{pol} are given by

$$\Sigma_i^{pol} = \frac{e}{2}\sum_\sigma \int \psi_i^*(\mathbf{r},\sigma) V_S(\mathbf{r}) \psi_i(\mathbf{r},\sigma)\, d\mathbf{r} \quad (11)$$

where $V_S(\mathbf{r}) = \lim_{\mathbf{r}'\to\mathbf{r}}[G(\mathbf{r},\mathbf{r}') - G_{bulk}(\mathbf{r},\mathbf{r}')]$. Here $G(\mathbf{r},\mathbf{r}')$ is the Green's function associated with the Poisson equation, and $G_{bulk}(\mathbf{r},\mathbf{r}')$ is the bulk Green's function. We use the analytical expression of $V_S(\mathbf{r})$ for a spherical quantum dot[11] of radius R and dielectric constant ϵ_{in} embedded in a medium of dielectric constant ϵ_{out}. Because of the discontinuity of $\epsilon(\mathbf{r})$ at the surface of the dot, $V_S(\mathbf{r})$ has a nonintegrable singularity for $r = R$, which is removed by applying a smoothing function $1 - e^{-(r-R)^2/\sigma^2}$, where σ is a broadening factor of the order of the bond length.

We consider here InAs spherical nanocrystals of diameter $D = 30.3$ and 42.2 Å. The surface dangling bonds are passivated using a large-gap barrier material.[14] Our analysis of the envelope functions extracted from the pseudopotential wave functions shows that the first electron level (e1) is predominantly s-like, while the next three electron levels (e2, e3, and e4) are predominantly p-like. The first two hole levels (h1 and h2) have an s-like envelope function, while the next two hole levels (h3 and h4) have a p-like envelope function. Each single-particle energy level is doubly degenerate because of time-reversal symmetry.

The self-energies Σ_i^{pol}, the polarization energies $J_{i,j}^{pol}$, and the direct Coulomb energies $J_{i,j}^{dir}$ of the 30.3 Å diameter InAs nanocrystal are shown in Figure 2 as a function of the external dielectric constant ϵ_{out}, for a few single-particle states i and j.

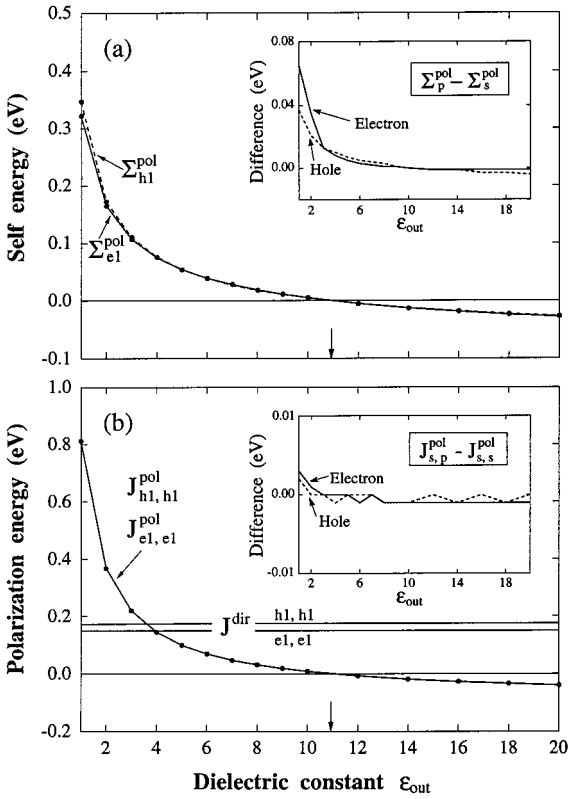

Figure 2. Self-energies Σ^{pol}_{h1} and Σ^{pol}_{e1} (a) and polarization energies $J^{pol}_{h1,h1}$ and $J^{pol}_{e1,e1}$ (b) of an InAs quantum dot (diameter $D = 30.3$ Å) shown as a function of the outside dielectric constant ϵ_{out}. Also shown in (b) are the direct Coulomb energies $J^{dir}_{h1,h1}$ and $J^{dir}_{e1,e1}$. The insets show the differences $\Sigma^{pol}_{p} - \Sigma^{pol}_{s}$ and $J^{pol}_{s,p} - J^{pol}_{s,s}$ as a function of ϵ_{out}. The vertical arrows indicate the value $\epsilon_{out} = \epsilon_{in}$.

We see that (i) both Σ^{pol}_{i} and $J^{pol}_{i,j}$ depend strongly on ϵ_{out} and vanish when $\epsilon_{out} = \epsilon_{in}$ (vertical arrows in Figure 2); (ii) when $\epsilon_{out} > \epsilon_{in}$ the polarization energies $J^{pol}_{i,j}$ become negative, thus acting to diminish the electron−electron interaction; (iii) the dependence of Σ^{pol}_{i} and $J^{pol}_{i,j}$ on the identity of the orbitals i and j (e.g., s or p) is rather weak, as shown in the insets in Figure 2; (iv) there is a critical value of ϵ_{out} ($\epsilon_{critical} \sim 4$) such that for $\epsilon_{out} < \epsilon_{critical}$ the polarization energies $J^{pol}_{i,j}$ dominate over the direct Coulomb energies $J^{dir}_{i,j}$.

The charging energies $\mu_N = E_N - E_{N-1}$, calculated from the total energies E_N given by eq 7, are shown in the central panel of Figure 3 as a function of ϵ_{out}. The vertical arrow at the bottom of the figure denotes the value $\epsilon_{out} = \epsilon_{in}$, which divides the behavior into two domains: (i) In the weak screening regime ($\epsilon_{out} \ll \epsilon_{in}$) the charging energies are widely spaced, and their value depends strongly on ϵ_{out}. (ii) In the strong screening regime ($\epsilon_{out} \geq \epsilon_{in}$) the charging energies are closely spaced and do not depend significantly on ϵ_{out}. The calculated charging spectrum is shown in Figure 3 for $\epsilon_{out} = 1$ (left-hand side) and $\epsilon_{out} = 20$ (right-hand side), illustrating these two limiting behaviors.

The electron and hole addition energies $\Delta_{N,N+1}$ (spacings between peaks in the charging spectra of Figure 3), the quasiparticle gap ϵ^{qp}_{gap}, and the optical gap ϵ^{opt}_{gap} are summarized in Table 1 for a few values of ϵ_{out}.

Electron Addition Energies. We see from Table 1 that the addition energy of the third electron $\Delta^{(e)}_{2,3}$ is significantly larger than the addition energy of the second electron $\Delta^{(e)}_{1,2}$. This can be explained by noting from eqs 4 and 5 that while $\Delta^{(e)}_{1,2}$ measures only the interelectronic repulsion, $\Delta^{(e)}_{2,3}$ includes also the single-particle gap $\epsilon_{e2} - \epsilon_{e1}$ between the s-like state e1 and the p-like states e2, e3, and e4. We find $\epsilon_{e2} - \epsilon_{e1} = 400$ meV for the 30.3 Å diameter nanocrystal and 360 meV for the 42.2 Å diameter nanocrystal. The addition energies of the remaining electrons (up to $N = 8$) are approximately constant, as a consequence of the fact that the p-like states e2, e3, and e4 are nearly degenerate. The addition energy of the ninth electron, $\Delta^{(e)}_{8,9}$, is slightly larger, and reflects the single-particle gap between the p-like shell and the next (d-like) shell.

Hole Addition Energies. The addition energies of the holes are approximately constant. This is due to the fact that the energy difference between the h1, h2 and the h3, h4 single-particle states is relatively small (38 meV in the 30.3 Å diameter nanocrystal and 14 meV in the 42.2 Å diameter nanocrystal) and is comparable with the variations of the direct Coulomb energies $J^{dir}_{i,j}$ between different hole states. Banin et al.[1] found

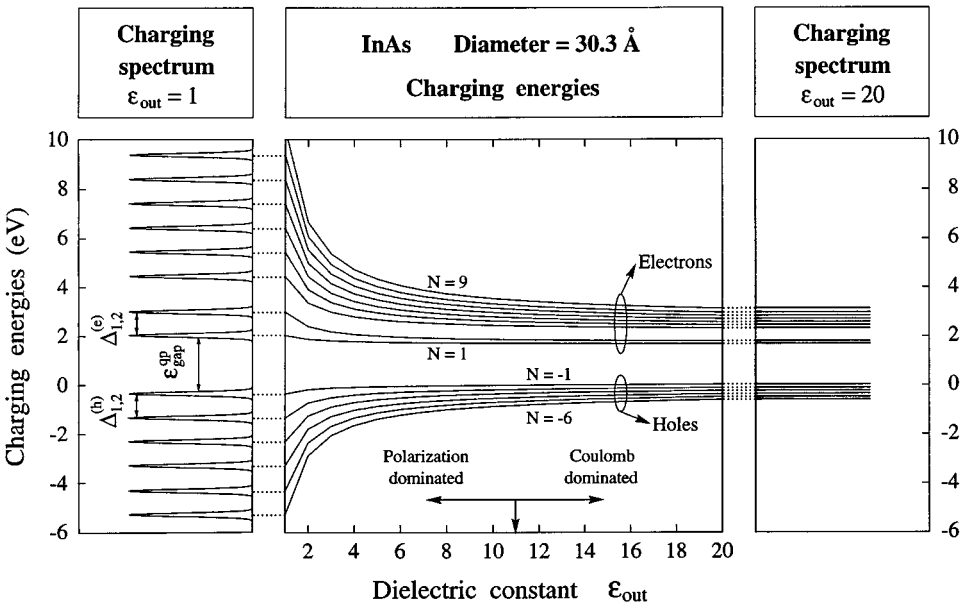

Figure 3. (middle panel) Dependence of the electron and hole charging energies on the outside dielectric constant ϵ_{out}. The vertical arrow indicates the value $\epsilon_{out} = \epsilon_{in}$. The side panels show the calculated charging spectrum in the case $\epsilon_{out} = 1$ (left-hand panel) and $\epsilon_{out} = 20$ (right-hand panel). The zero of the energy scale corresponds to the highest-energy valence state.

TABLE 1: Addition Energies $\Delta_{N,N+1}$, Quasi-Particle Gap ϵ_{gap}^{qp}, and Optical Gap ϵ_{gap}^{opt} of InAs Nanocrystals (in eV) for Different Values of the Dielectric Constant ϵ_{out}

	$D = 30.3$ Å, $\epsilon_{gap} = 1.71$ eV				$D = 42.2$ Å, $\epsilon_{gap} = 1.31$ eV			
$\epsilon_{out} =$	1	6	10	20	1	6	10	20
				Electrons				
$\Delta_{1,2}^{(e)}$	0.96	0.22	0.16	0.11	0.69	0.15	0.10	0.07
$\Delta_{2,3}^{(e)}$	1.45	0.64	0.57	0.53	1.05	0.51	0.46	0.43
$\Delta_{3,4}^{(e)}$	0.98	0.24	0.17	0.13	0.70	0.15	0.10	0.07
$\Delta_{4,5}^{(e)}$	0.99	0.24	0.18	0.13	0.69	0.15	0.10	0.07
$\Delta_{5,6}^{(e)}$	0.98	0.24	0.17	0.13	0.67	0.14	0.09	0.06
$\Delta_{6,7}^{(e)}$	0.98	0.23	0.17	0.13	0.71	0.16	0.11	0.08
$\Delta_{7,8}^{(e)}$	0.99	0.24	0.18	0.13	0.68	0.14	0.10	0.07
$\Delta_{8,9}^{(e)}$	1.03	0.28	0.21	0.17				
$\Delta_{9,10}^{(e)}$	1.00	0.25	0.19	0.14				
				Holes				
$\Delta_{1,2}^{(h)}$	0.98	0.23	0.17	0.13	0.73	0.18	0.13	0.10
$\Delta_{2,3}^{(h)}$	1.04	0.26	0.19	0.14	0.68	0.15	0.10	0.07
$\Delta_{3,4}^{(h)}$	0.97	0.22	0.16	0.11	0.73	0.17	0.13	0.09
$\Delta_{4,5}^{(h)}$	0.91	0.21	0.15	0.11	0.68	0.15	0.11	0.07
$\Delta_{5,6}^{(h)}$	1.03	0.24	0.17	0.12	0.73	0.17	0.12	0.09
				Gaps				
ϵ_{gap}^{qp}	2.37	1.78	1.72	1.65	1.84	1.38	1.32	1.27
ϵ_{gap}^{opt}		1.56	1.55	1.54		1.22	1.21	1.20

two distinct multiplets in the hole addition spectrum, which they denoted as 1_{VB} and 2_{VB}. They attributed the 2_{VB} multiplet to tunneling of holes into the $2S_{3/2}$ valence-band level. We find that the $2S_{3/2}$ level is significantly lower in energy than the h1−h4 levels, so we do not consider hole injection into the $2S_{3/2}$ level. Our calculations show that charging of the h1−h4 levels produces a rather featureless spectrum, and that the first multiplet in the hole addition spectrum (1_{VB}) consists of at least eight nearly equally spaced peaks. The fact that Banin et al.[1] do not observe such a high multiplicity suggests that some of the hole charging peaks may be missing.

Quasi-Particle and Optical Gap. As shown in Table 1, the quasi-particle gap ϵ_{gap}^{qp} depends strongly on ϵ_{out}, while the optical gap $\epsilon_{gap}^{opt} = \epsilon_{gap}^{qp} - J_{h1,e1}$ does not. This is so because the terms $(\Sigma_{h1}^{pol} + \Sigma_{e1}^{pol})$ and $J_{h1,e1}^{pol}$ tend to cancel, so $\epsilon_{gap}^{opt} \sim (\epsilon_{e1} - \epsilon_{h1}) - J_{h1,e1}^{dir}$.

Table 1 provides clear predictions for the addition energies and the quasi-particle gap of InAs nanocrystals. To compare with the experimental measurements of Banin et al. (ref 1), in which ϵ_{out} is an unknown quantity, we first fit our calculated $\Delta_{1,2}^{(e)}$ for the smaller dot with the experimental value $\Delta_{1,2}^{(e)} = 0.22$ eV, finding that $\epsilon_{out} = 6$ gives a good fit (Table 1). This value of ϵ_{out} should be viewed as the "effective" dielectric constant of the environment, which accounts for the presence of metal electrodes as well as organic ligands. Using $\epsilon_{out} = 6$, we then predict for $D = 30.3$ Å (experimental data in parentheses for $D = 34$ Å) $\epsilon_{gap}^{qp} = 1.78$ (1.75), $\Delta_{1,2}^{(h)} = 0.23$ (0.20), $\Delta_{2,3}^{(h)} = 0.26$ (0.22), $\Delta_{2,3}^{(e)} = 0.64$ (0.71), and $\Delta_{3,4}^{(e)} = 0.24$ (0.23). Using the same value of ϵ_{out}, our predictions for $D = 42.2$ Å (experimental data in parentheses for $D = 44$ Å) are: $\epsilon_{gap}^{qp} = 1.38$ (1.38), $\Delta_{1,2}^{(h)} = 0.18$ (0.20), $\Delta_{2,3}^{(h)} = 0.15$ (0.17), $\Delta_{1,2}^{(e)} = 0.15$ (0.14), $\Delta_{2,3}^{(e)} = 0.51$ (0.52), and $\Delta_{3,4}^{(e)} = 0.15$ (0.14). We see that we can achieve a very good agreement with experiment using a single value of the parameter ϵ_{out}.

Our theory can be further used to decompose the experimentally measured quantities into distinct physical contributions. For example, for $D = 30.3$ Å the quasi-particle gap $\epsilon_{gap}^{qp} = 1.78$ eV includes [eq 6] the single-particle gap $\epsilon_{e1} - \epsilon_{h1} = 1.71$ eV and the polarization self-energy contribution $\Sigma_{h1}^{pol} + \Sigma_{e1}^{pol} = 0.07$ eV. The addition energy for the third electron $\Delta_{2,3}^{(e)} = 0.64$ eV includes [eq 5] the single-particle contribution $\epsilon_{e2} - \epsilon_{e1} = 0.40$ eV, the direct Coulomb contribution $2J_{e1,e2}^{dir} - J_{e1,e1}^{dir} = 0.17$ eV, the polarization contribution $2J_{e1,e2}^{pol} - J_{e1,e1}^{pol} = 0.07$ eV, and a negligible self-energy contribution $\Sigma_{e2}^{pol} - \Sigma_{e1}^{pol}$. The exchange contribution $K_{e1,e2}$ is smaller than 0.02 eV, and can be neglected.

In conclusion, we predict the effects of the dielectric environment on the electron and hole charging energies and on the addition spectrum of semiconductor quantum dots. We find that the charging energies and the addition energies depend sensitively on the dielectric constant ϵ_{out} of the surrounding material via the self-energies Σ_i^{pol} and the polarization energies $J_{i,j}^{pol}$. Our calculations for InAs nanocrystals are in excellent agreement with recent spectroscopic results[1] for $\epsilon_{out} = 6$, and provide a quantitative prediction of how single-electron tunneling in quantum dots can be tuned by changing the dielectric environment.

This work was supported by the U.S. DOE, Office of Science, Division of Materials Science, under Grant No. DE-AC36-98-GO10337.

References and Notes

(1) Banin, U.; Cao, Y.; Katz, D.; Millo, O. *Nature* **1999**, *400*, 542.
(2) Keldysh, L. V. *Pis'ma Zh. Eksp. Teor. Fiz.* **1979**, *29*, 716; *JETP Lett.* **1979**, *29*, 658.
(3) Brus, L. E. *J. Chem. Phys.* **1983**, *79*, 5566; **1984**, *80*, 4403.
(4) Murray, C. B.; Norris, D. J.; Bawendi, M. G. *J. Am. Chem. Soc.* **1993**, *115*, 8706.
(5) Leonard, D., et al. *Appl. Phys. Lett.* **1993**, *63*, 3203.
(6) Alivisatos, A. P. *Science* **1996**, *271*, 933.
(7) Tarucha, S., et al. *Phys. Rev. Lett.* **1996**, *77*, 3613.
(8) Sopanen, M.; Lipsanen, H.; Ahopelto, J. *Appl. Phys. Lett.* **1995**, *66*, 2364.
(9) Ekimov, A. *J. Lumin.* **1996**, *70*, 1.
(10) Babic, D.; Tsu, R.; Greene, R. F. *Phys. Rev. B* **1992**, *45*, 14150.
(11) Banyai, L.; Gilliot, P.; Hu, Y. Z.; Koch, S. W. *Phys. Rev. B* **1992**, *45*, 14136.
(12) Lannoo, M.; Delerue, C.; Allan, G. *Phys. Rev. Lett.* **1995**, *74*, 3415.
(13) Goldoni, G.; Rossi, F.; Molinari, E. *Phys. Rev. Lett.* **1998**, *80*, 4995.
(14) Williamson, A.; Zunger, A. *Phys. Rev. B* **2000**, *61*, 1978.
(15) Franceschetti, A.; Zunger, A. *Phys. Rev. Lett.* **1997**, *78*, 915.
(16) Franceschetti, A.; Fu, H.; Wang, L. W.; Zunger, A. *Phys. Rev. B* **1999**, *60*, 1819.
(17) Rontani, M.; Rossi, F.; Manghi, F.; Molinari, E. *Phys. Rev. B* **1999**, *59*, 10165.